NIH Public Access
Author Manuscript
Mol Pharm. Author manuscript; available in PMC 2010 September 1.

Published in final edited form as:
Mol Pharm. 2009 ; 6(5): 1506–1517. doi:10.1021/mp900081y.

Galactosylated LDL nanoparticles:

a novel targeting delivery system to deliver antigen to macrophages and enhance antigen specific T cell responses

Fang Wu[*,+], **Sherry A. Wuensch**, **Mitra Azadniv**, **Mohammad R. Ebrahimkhani**[□], and **I. Nicholas Crispe**[□]
David H. Smith Center for Vaccine Biology and Immunology, The Aab Institute for Biomedical Research, Department of Microbiology and Immunology, University of Rochester Medical Center, Rochester, NY 14642

Abstract

We aim to define the role of Kupffer cells in intrahepatic antigen presentation, using the selective delivery of antigen to Kupffer cells rather than other populations of liver antigen-presenting cells. To achieve this we developed a novel antigen delivery system that can target antigens to macrophages, based on a galactosylated low-density lipoprotein nano-scale platform. Antigen was delivered via the galactose particle receptor (GPr), internalized, degraded and presented to T cells. The conjugation of fluoresceinated ovalbumin (FLUO-OVA) and lactobionic acid with LDL resulted in a substantially increased uptake of FLUO-OVA by murine macrophage-like ANA1 cells in preference to NIH-3T3 cells, and by primary peritoneal macrophages in preference to primary hepatic stellate cells. Such preferential uptake led to enhanced proliferation of OVA specific T cells, showing that the galactosylated LDL nano-scale platform is a successful antigen carrier, targeting antigen to macrophages but not to all categories of antigen presenting cells. This system will allow targeted delivery of antigen to macrophages in the liver and elsewhere, addressing the question of the role of Kupffer cells in liver immunology. It may also be an effective way of delivering drugs or vaccines directly at macrophages.

Keywords

antigen delivery system; fluorescence conjugated ovalbumin; LDL; nano-scale platform; galactose particle receptor; macrophages; proliferation of T cells

Introduction

Kupffer cells (KCs) are the largest population of macrophages, and account for about 20% of non-parenchymal cells in the liver[1].Other non-parenchymal cell populations include liver sinusoidal endothelial cells (LSEC), biliary epithelial cells, hepatic stellate cells (HSC) and intrahepatic lymphocytes. Parenchymal cells, known as hepatocytes, constitute the remainder, making up about two thirds of the total liver cells[2]. Several liver cell populations may contribute to activation of naive T lymphocytes within the liver. When naive T lymphocytes recirculate within the liver sinusoids, they may be activated by contact with KC or LSEC located within the lumen of the sinusoids, or by contact through the gap between two adjacent LSEC, or may

[*]Corresponding author. fwu5@buffalo.edu
[+]Current address: Department of Pharmaceutical Sciences, School of Pharmacy and Pharmaceutical Sciences, University at Buffalo, State University of New York, Amherst, NY 14260
[□]Current Address: Seattle Biomedical Research Institute, 307 North Westlake Avenue, Seattle, WA 98119

NIH-PA Author Manuscript
NIH-PA Author Manuscript
NIH-PA Author Manuscript

NIH-PA Author Manuscript

NIH-PA Author Manuscript

NIH-PA Author Manuscript

interact via fenestrations in the LSEC with stellate cells in the space of Disse, or with hepatocytes[3]. To facilitate the analysis of antigen presentation by KC in the liver, we created an antigen delivery system targeting macrophages. We specifically compared antigen delivery to macrophages versus hepatic stellate cells, since these cells are also powerful antigen presenting cells (APC). This delivery system could also be used as a drug delivery system, for example delivering drugs such as a TNF-α (Tumor Necrosis Factor-α) inhibitor to KC to reduce inflammation in hepatitis[4], or used as a vaccine delivery system to macrophages for generating an effective $CD8^+$ cytotoxic T-lymphocyte response.

When drugs or antigens are injected in soluble form, only a small fraction gains access to macrophages. To promote delivery of a drug or antigen to macrophages in the liver, various lipid and polymeric carriers such as liposomes[5], nanoparticles[6] and microspheres[7] have been used. In order to enhance the macrophage targeting properties, nanoparticles have been modified with the inclusion of ligands such as the mannose residue, mouse monoclonal antibody, fibronectin or galactose[8]. Such ligands have been conjugated with nanoparticles by a covalent modification through an amide bond [9, 10], by electrostatic interaction[11] or by biotin-streptavidin conjugation, allowing the binding of biotinylated ligands with streptavidin-coupled nanoparticles[12]. Macrophages take up such nanoparticles either by ligand-mediated, or by non-specific endocytosis[13, 14] and the drugs are released from the carriers following intra-lysosomal degradation of the carriers[8]. One common concern is the biocompatibility and immunogenicity of the delivery platforms which are not based on well-defined biological materials. Recently, Low Density Lipoprotein (LDL) has emerged as a candidate, as it is biocompatible, biodegradable and non-immunogenic. LDL nanoparticles may be modified, and targeted to deliver diagnostic, imaging or therapeutic agents to cancer cells [15, 16]. A lactose modified LDL, Tris-gal-chol-LDL, has also been used as a vehicle for the specific delivery of anti-parasitic or antiviral drugs to infected KCs[17] and Bijsterbosch et al also prepared lactosylated LDL by reductive lactosamination to deliver oligodeoxynucleotide to KCs[18], which possess galactose particle receptor (GPr)[19]. Another modified LDL, acetylated LDL was specifically taken up by LSEC[20] and later was even used as a specific marker of LSEC[21]. Taken together, the lipoprotein family has good potential to be modified and used as carriers for targeting to different cell types in liver. The structure of lipoproteins features an apolar core surrounded by a shell composed of a phospholipid monolayer containing cholesterol and apolipoproteins (i.e. apolipoprotein B, apoB), and the amino acid residues of the proteins can be covalently conjugated with ligand, or with diagnostic or therapeutic agents[15].

In the present study, lysine residues of apo B on the LDL surface were randomly linked with the carboxylic acid ends of fluorescein conjugated OVA (FLUO-OVA) and the carboxylic acid end of lactobionic acid via carbodiimide chemistry, generating antigen loaded galactosylated LDL (GAL-LDL) nanoparticles, which we term FLUO-OVA-GAL-LDL. The conjugation of LDL with lactobionic acid generated terminal galactose residues, which resulted in targeting macrophages via the galactose receptor, following the approach of Bijsterbosch et al[18]. The internalized antigen could be detected by fluorescence generated from FLUO-OVA, and galactosylated LDL acted as a specific ligand for the GPr on macrophages. Both fluorescence microscopy and flow cytometry confirmed the enhanced uptake by macrophages of FLUO-OVA-GAL-LDL nanoparticles, compared to free FLUO-OVA nanoparticles. With increase of the galactosylation ratio, the OVA uptake via FLUO-OVA-GAL-LDL nanoparticles increased, leading to targeted delivery of antigen to macrophage-like ANA1 cells in preference to fibroblastic NIH3T3 cells. Of critical importance, this selective uptake was reproduced using primary ex vivo macrophages versus hepatic stellate cells. The mechanism of uptake by the macrophage was likely through the GPr mediated endocytosis pathway (Figure 1). OVA specific OT-1 T cells had significantly higher response when co-cultured with peritoneal macrophages pulsed with FLUO-OVA-GAL-LDL nanoparticles, versus FLUO-OVA. To date

NIH-PA Author Manuscript

NIH-PA Author Manuscript

NIH-PA Author Manuscript

there is no study indicating that galactosylated LDL is a successful antigen delivery system. Therefore, we believe that our study for the first time shows that the galactosylated LDL nano-scale platform is a successful antigen carrier, targeting antigen to macrophages but not to all categories of antigen presenting cells.

Experimental Section

Chemicals

Ovalbumin, fluorescein conjugate (45 kDa, FLUO-OVA), Carboxyfluorescein succinimidyl ester (CFSE) were obtained from Invitrogen Molecular Probes (Eugene, OR, USA) and Ovalbumin 257-264 peptide (SIINFEKL) was purchased from New England Peptide (Gardner, MA, USA). Low density lipoprotein (3,500kDa, LDL), lactobionic acid and N-Ethyl-N'-(3-dimethylaminopropyl) carbodiimide hydrochloride (EDC), DAPI (4′,6′-Diamidino-2-phenylindole dihydrochloride), 2-Mercaptoethanol were from Sigma-Aldrich (St. Louis, MO, USA). CellTiter 96® AQueous One Solution Reagent was purchased from Promega (Madison, WI, USA).

Cell lines

The murine macrophage-like cell line ANA1, and the murine embryonic fibroblast cell line NIH3T3, were obtained from ATCC (American Type Culture Collection, Manassas, VA, USA). All cells were grown in Dulbecco's modified Eagle's medium (DMEM, Invitrogen, Carlsbad, CA, USA), supplemented with 10% fetal bovine serum (FBS, Mediatech, Manassas, VA, USA), 100 units/mL penicillin-streptomycin (Mediatech, Manassas, VA, USA) and incubated at 37 □C in a humidified atmosphere containing 5% CO2.

Mice

Non-transgenic female C57BL/6J mice were purchased from the Jackson Laboratory (Bar Harbor, Maine, USA), for use as a source of primary peritoneal macrophages and hepatic stellate cells. Transgenic female C57BL/6-Tg (OT-1)-Thy1.1 mice were bred in house. All experiments were approved by the Institutional Animal Care and Use Committee.

Preparation of Fluorecein conjugated Ovalbumin loaded Galactosylated Low Density Lipoprotein (FLUO-OVA-GAL-LDL) nanoparticles

The carbodimide conjugation method via EDC was adapted from Yong, Xu and Gao et al[22-24]. Briefly, LDL was conjugated with FLUO-OVA and lactobionic acid via an active ester intermediate EDC. Briefly, 30 μL of 700 μg/mL FLUO-OVA in PBS solution and 30 μL of 2.79 mg/mL aqueous lactobionic acid solution were added to 146 μL of distilled water, Then 30 μL of 179 μg/mL aqueous EDC solution were added to this mixture to activate the carboxyl group on FLUO-OVA and lactobionic acid. After activation for 5 min at room temperature, 34 μL of LDL solution in 150 mM NaCl, pH7.4, and 0.01% EDTA (Sigma, St. Louis, MO, USA) was added to this solution and reacted overnight at 4 °C, and then the FLUO-OVA-Galactosylated LDL (FLUO-OVA-GAL-LDL) nanoparticles colloid solution was obtained. The molar ratio of FLUO-OVA/LA/LDL/EDC in this reaction was 10:5000:1:600 or otherwise indicated in the article. Unbound FLUO-OVA and excess linking reagent EDC were removed by centrifugation at 14,000×g at 4°C for 2 h and the precipitated antigen loading nanoparticles were re-dispersed in appropriate amount of PBS and the loaded OVA content was determined by fluorescence assay.

NIH-PA Author Manuscript

NIH-PA Author Manuscript

NIH-PA Author Manuscript

Fluorescence assay to determine the loaded OVA content and calculation of drug loading and loading efficiency

The loaded FLUO-OVA content was quantified by measuring the fluorescence intensity of fluorescein with excitation at 490 nm and detection at 520 nm using a Spectra Max Gemini Microplate Spectrofluorometer (Molecular Devices, Sunnyvale, CA, USA)[25]. A calibration curve of standard FLUO-OVA in PBS was used to determine the concentration of FLUO-OVA in the FLUO-OVA-GAL-LDL nanoparticle colloid PBS solution. The curve was linear over the range of 1-200 μg/mL with a correlation coefficient of R^2=0.9994. The loaded OVA concentration on FLUO-OVA-GAL-LDL was derived from the calibration curve. The drug loading of the nanoparticles and loading efficiency (LE) were calculated from the following equation: DL=M1/M2×100%, LE=M1/M3×100%, where M1 is the weight of FLUO-OVA loading on LDL nanoparticle, M2 is the weight of LDL nanoparticles added, and M3 is the total weight of FLUO-OVA used in the preparing process. Each experiment was carried out in triplicate.

Characterization of nanoparticles

Morphology and size of nanoparticles was determined using Transmission Electron Microscopy (TEM). A HITACHI 7650 Transmission Microscope equipped with a Cecetan digital camera was used to determine the morphology and the size of the aqueous dispersion of nanoparticles. Twenty μL of lipoprotein nanoparticle suspension was placed on 200-mesh nickel grids and allowed to stand for 2 min. Excess sample was removed with filter paper, and 20 μL of filtered 2% saturated phosphotungstic acid was applied to the grid. The stain was then drained off with filter paper, and the grid was air-dried (about 5 min) before digital images were taken.

Particle sizes were also measured using a dynamic light scattering (DLS) particle sizer (Malvern Z-sizer, Malvern Instruments, Malvern, UK). Briefly, 5 μL of the nanoparticle conjugation solution (molar ratio of FLUO-OVA:LA:LDL:EDC is 10:5000:1:600) or 5 μL of native LDL nanoparticles is diluted in 1 mL of distilled water at 25 □C and the Z-average value reported by the software provided by the manufacturer is the mean diameter of the particles. All measurements were made in triplicate.

Cytotoxicity Assay

To assess cell viability, the CellTiter 96® nonradioactive MTS-based cell proliferation assay (CellTiter 96® AQueous One Solution Reagent) was applied[26, 27]. The colorimetric MTS assay is based on the selective ability of living cells to reduce 3-(4, 5-dimethylthiazol-2-yl)-5-(3-carboxymethoxyphenyl)-2-(4-sulfophenyl)-2H-tetrazolium bromide into a colored formazan product that is soluble in cell culture medium. The quantity of produced formazan was measured by recording the absorbance at 490 nm, which is directly proportional to the number of living cells.

To test the cytotoxicity of the nanoparticles, 1×10^4 ANA1 cells or NIH3T3 cells per well of a 96-well plate were incubated with various amount of FLUO-OVA-GAL-LDL nanoparticles in 100 μL of DMEM medium without phenol red (Invitrogen, Carlsbad, CA, USA), supplemented with 10% FBS and 100 units/mL penicillin-streptomycin for 24h. Then 20 μL of CellTiter 96® AQueous One Solution Reagent was added into each well, followed by further incubation for 2h at 37 °C. The relative viability of the cells incubated with nanoparticles or free FlUO-OVA to untreated cells was determined by measuring the MTS-formazan absorbance on a Kinetic microplate reader (Vmax, Molecular Devices, Sunnyvale, CA, USA) at 490 nm with a subtraction of the absorbance of cell-free blank volume at 490 nm indicated as following formula. The results from three individual experiments were averaged.

NIH-PA Author Manuscript

NIH-PA Author Manuscript

NIH-PA Author Manuscript

$$\text{Cell viability (\%)} = \frac{\text{Abs sample} - \text{Abs background1}}{\text{Abs control} - \text{Abs background2}} \times 100$$

Where Abs sample is the absorbance of the cells incubated with the samples and Abs background1 is the absorbance of cell-free well with only media and samples. Abs control is the absorbance of the cells incubated with only media and Abs background 2 is the absorbance of cell-free well with only media.

Isolation of primary peritoneal macrophages and hepatic stellate cells

Mouse peritoneal macrophages were isolated as described[28] with some modification. Briefly, seven-to-twelve-week-old female C57BL/6J mice were sacrificed and the peritoneum was exposed, then the mice were injected intraperitoneally (i.p.) with 3 mL of ice-cold PBS supplemented with 5% heat-inactivated FBS. The abdomen was agitated gently and the media were removed using the same syringe. The cell suspension was centrifuged at 800×g for 10 min and the pellet was resuspended in DMEM media supplemented with 10% FBS and 100 units/mL penicillin-streptomycin. The peritoneal macrophages suspension was seeded in a 24-well culture plate at 2×10^5 cells per well in 1 mL. The macrophages were allowed to adhere for 48 hours before removing the media containing non-adherent cells and replacing with new media. More than 90% of the attached cells were CD11b positive as confirmed by flow cytometry. Hepatic stellate cells (HSC) were isolated from the liver of normal female C57BL/6 mice as described previously with some modifications [29]. Briefly, the liver was perfused in situ by pronase and collagenase solutions followed by discontinuous density centrifugation in 11.5% Optiprep (Axis shield, Oslo, Norway, USA). The HSCs fraction located at the top of the Optiprep layer was gently aspirated and cultured in DMEM supplemented with 16% fetal calf serum (FCS, Mediatech, Manassas, VA, USA) and 100 units/mL penicillin-streptomycin. After 24 hours, non-adherent cells and debris were removed by washing with media. One day before the experiments, HSC were trypsinized using GIBCO 0.25% Trypsin-EDTA (Invitrogen, Carlsbad, CA, USA) and seeded in 24-well plate at a density of 2×10^5 cells per well.

Cell targeting and qualitative uptake study of FLUO-OVA-GAL-LDL nanoparticles by fluorescent microscopy

ANA1 cells were plated at 1×10^5 cells per well on an 8-well Lab-Tek chamber slide, NIH 3T3 cells were plated at 5×10^4 cells per well due to its rapid growing rate. Cells were grown for at least 12 h in the 8-well Lab-Tek chamber slide before uptake experiments. Experiments were initiated by adding 50 μL of FLUO-OVA-GAL-LDL nanoparticles colloid solution in PBS (reaction molar ratio of FLUO-OVA: LA: LDL: EDC is 10:500:1:600) or adding 4.4 μL of 700 μg/mL of free FLUO-OVA in PBS solution per well with 300 μL culture medium to obtain a final concentration of 10 μg/mL of FLUO-OVA. After 5 h of incubation at 37 □C, cells were washed three times with 200 μL ice-cold PBS and then fixed for 20 min with 4% paraformaldehyde (Electron Microscopy Sciences, Fort Washington, PA, USA) in PBS at room temperature. Then the cells were rinsed twice with PBS and 200 μL of 100 ng/mL of DAPI aqueous solution was added for nuclei staining at 4 □C overnight until Zeiss Axiovert Microscope assay. The Zeiss Axiovert Microscope (Carl Zeiss MicroImaging, Inc., Thornwood, NY, USA) was controlled by SlideBook software (Intelligent Imaging Innovations, Inc., Denver, CO, USA) and the fluorescence emissions of fluorescein and DAPI were observed using FITC and DAPI filter sets, respectively. Fluorescent images were obtained at 40× magnification.

NIH-PA Author Manuscript

NIH-PA Author Manuscript

NIH-PA Author Manuscript

Cell targeting and quantitative uptake study of FLUO-OVA-GAL-LDL nanoparticles by flow cytometry

ANA1 cells or NIH3T3 cells were seeded at 2×10^5 cells per well in a 24-well plate and allowed to grow overnight. Primary cells (peritoneal macrophages or hepatic stellate cells) were isolated and seeded as described above. Then cells were incubated with different formulation of FLUO-OVA-GAL-LDL or free FLUO-OVA at predetermined concentrations as indicated in the figure legends at 37 □C for 5 hours. At the conclusion of each experiment, cells were washed three times with PBS to remove the FLUO-OVA-GAL-LDL nanoparticles or free FLUO-OVA which have not been taken up. Cells were then trypsinized, added with 1 mL media and centrifuged at 800×g to remove the trypsin, then re-suspended in PBS with 2% paraformaldehyde before analysis by flow cytometry. A FACScan (BD Biosciences, San Jose, CA, USA) instrument and CellQuest software (BD Biosciences, San Jose, CA, USA) were used to assess fluorescence. Ten thousand cells per FACS tube were excited at 488 nm and fluorescence was detected at 530 nm. Control cells incubated with PBS were used to correct for nonspecific cellular fluorescence.

Mechanistic study of uptake of FLUO-OVA-GAL-LDL nanoparticles

ANA1 cells were seeded at a density of 3×10^5 cells per well on a 24-well plates, cells were allowed to grow at 37 □C in a humidified atmosphere with 5% CO2 overnight. Cells were pre-incubated with PBS, 60 μL of GAL-LDL PBS suspension (self-conjugated using the similar method as described for FLUO-OVA-GAL-LDL conjugation, the reaction amounts of lactobionic acid and LDL are 10 fold of those in the preparation of FLUO-OVA-GAL-LDL), 100 μL of 4mg/mL of LDL colloid solution (10-fold excess of LDL) for 45 min at 37 □C. Then cells were washed twice with media to get rid of pre-treated materials and change with new media and FLUO-OVA-GAL-LDL nanoparticles or equivalent concentration of OVA were added to the treated cell culture to get the final OVA concentration of 1.5 μg/mL and incubated for 5 h. At the end of the incubation, the media containing nanoparticles or free OVA was removed and the ANA1 cell monolayer was washed three times with media. Subsequently, cells were harvested and fluorescence generated by the internalized FLUO-OVA was examined by flow cytometry using a FACScan.

Antigen presentation study

To test antigen presentation[30], peritoneal macrophages were used because they are commonly used model macrophages in such experiments[31, 32] and are easier to be isolated than KC. Peripheral lymph nodes and spleen from seven-to-twelve-week-old female OT-1 T cell receptor transgenic mice were homogenized using frosted glass slides, filtered through a 100 μm cell strainer, washed and resuspended in 5 mL of PBS supplemented with 5% FBS. Lymphocytes from this cell suspension were isolated by density gradient centrifugation (Lympholyte-M; Cedarlane Laboratories, Ontario, Canada). Briefly, 5 mL of the cell suspension was layered over 5 mL of lympholyte-M, and centrifuged at 1500×g for 20 min at room temperature. The lymphocytes at the interface were collected, washed with PBS and counted. For CFSE labeling, lymphocytes were resuspended in 2.5 mL of PBS supplemented with 5% FBS, mixed with 2.5 mL of PBS containing 2 μM CFSE. Cells were stained with CFSE for 10 min at 37 □C, and then washed with PBS.

The peritoneal macrophages cultured in 24-well plate were stimulated with LDL, free FLUO-OVA in PBS or FLUO-OVA-GAL-LDL (reaction molar ratio of FLUO-OVA: Lactobionic acid: LDL: EDC=150:5000:1:600) nanoparticles colloid solution in PBS at a predetermined FLUO-OVA concentration, or stimulated with 1.5 μg/mL of OVA Peptide SIINFEKL as a positive control and PBS as a negative control. After 14 hours, media were removed and washed twice with media and replaced with RPMI 1640 containing 10% FBS, 100 units/mL penicillin-streptomycin and 50 μM 2-mercaptoethanol. After 5 hours, 1×10^6 CFSE labeled lymphocytes

NIH-PA Author Manuscript

NIH-PA Author Manuscript

NIH-PA Author Manuscript

from OT.1 mice were added to the peritoneal macrophages cultures. On day 5 of co-culture, non-adherent lymphocytes were harvested and stained for flow cytometry to analyze their proliferation. Proliferations were detected as dilution of CFSE on OT.1 CD8 T cells as gated on $V\alpha2^+CD8^+$ cells. Briefly, harvested lymphocytes were resuspended in staining solution (5% FBS in PBS) and incubated with antibodies (Abs, 1:500) against cell surface markers. Abs used for flow analysis were anti-Vα2 (PE) and anti-CD8 (PerCP), and these were purchased from BD Biosciences. Flow cytometric data were acquired using a FACScan flow cytometer. Analysis was performed using FlowJo cytometry analysis software (Tree Star, Inc., Ashland, OR, USA) on a Macintosh computer. Live lymphocytes were identified based on forward and side scatter.

Statistical Analysis

Data were expressed as the mean±SD. The significance of differences was analyzed using the one-way ANOVA test. A *P* value of less than 0.05 was considered significant.

Results and Discussion

Preparation, Characterization and Cytotoxicity of FLUO-OVA-GAL-LDL Nanoparticles

The LDL is an appealing nano-scale delivery carrier, because these particles are biocompatible, biodegradable, and non-immunogenic. Such LDL nanoparticles have been used to deliver diagnostic, imaging or therapeutic agents to cancer cells[15, 16]. To further investigate the potential of LDL as an antigen delivery system which could target specific antigen presenting cells, we prepared antigen loaded galactosylated LDL (GAL-LDL), FLUO-OVA-GAL-LDL nanoparticles by randomly linking the surface of LDL with the carboxylic acid ends of fluorescein conjugated OVA (FLUO-OVA) and the carboxylic acid end of lactobionic acid via carbodiimide chemistry. The internalized antigen could be detected by fluorescence generated from FLUO-OVA, and the galactosylated LDL acted as a specific ligand for the GPr receptor on macrophages.

The scheme for the conjugation of FLUO-OVA-GAL-LDL is outlined in Figure 2. In order to develop an antigen delivery system able to target a desired set of cells, the binding procedure must preserve the biological activity of antigen and maintain the structure and the activity of the ligand. N-Ethyl-N'-(3-dimethylaminopropyl) carbodiimide hydrochloride (EDC) has been used for covalent binding of antibody or transferrin to the surface of nanoparticles, with retention of their activity[22, 23]. Similarly, EDC has been used for covalently binding the carboxylic acid end of lactobionic acid with the primary amine end of low molecular weight chitosan (LMWC) to achieve galactosylated LMWC and the galactosylation degree increased linearly with the increase of LA/LMWC molar ratio[24]. The Apo B-100 protein of LDL is among the largest proteins known, with 4,536 amino acids and a molecular mass of 550 kDa, which provides a large amount of primary amine to be chemically modified[15]. Thus, in our study, EDC was used to conjugate the primary amine group on the Apo B of LDL particles with the free carboxylic end group of FLUO-OVA and lactobionic acid, forming a connecting amide bond. Excess reagent and the isourea formed as the by-product of the cross-linking reaction are both water-soluble and can easily be removed by centrifugation.

Transmission electron microscopy (TEM) revealed the morphology of native LDL (Figure 3A) and of FLUO-OVA-GAL-LDL nanoparticles (Figure 3B). TEM measurements showed that FLUO-OVA-GAL-LDL nanoparticle diameters are around 27 nm and native LDL are approximately 22 nm, n=10 for each sample. Dynamic light scattering (DLS) measurement estimated the mean diameter of the particles as 20.6±4.52 nm for native LDL and 23.2 ± 3.89 nm for FLUO-OVA-GAL-LDL nanoparticles, respectively, confirming the TEM measurements. This suggests that there was no significant coalescence during the covalently

NIH-PA Author Manuscript

NIH-PA Author Manuscript

NIH-PA Author Manuscript

binding of FLUO-OVA and galactosylated moiety to LDL nanoparticles. The unbound FLUO-OVA and excess linking reagent EDC were removed by centrifugation at 14,000×g at 4 □C for 2 hours, the precipitated antigen loading nanoparticles were re-dispersed in appropriate amount of 1×PBS, and the loaded OVA content on FLUO-OVA-GAL-LDL nanoparticles was determined by fluorescence assay. When the molar conjugation ratio of OVA: lactobionic acid: LDL: EDC was taken as 10:5000:1:600, the drug loading of the nanoparticles and loading efficiency (LE) are 2.18% ±0.04% and 14.11% ±0.28%, respectively. In addition, DLS was used to monitor the colloidal stability of the FLUO-OVA-GAL-LDL nanoparticles dispersed in phosphate buffered saline (pH 7.4). There was no significant change in hydrodynamic diameter before and after resuspension.

To measure the cytotoxicity of these antigen loaded nanoparticles, we measured cellular metabolic activity by using the CellTiter 96® nonradioactive MTS-based cell proliferation assay (CellTiter 96® AQueous One Solution assay kit) 24 h post-incubation with free FLUO-OVA or FLUO-OVA-GAL-LDL nanoparticles at an FLUO-OVA concentration up to 22 μg/mL. The MTS in vitro cytotoxicity assay is a convenient method for assessing cell viability which is used extensively due to its ease of use, accuracy and rapid indication of toxicity[26, 33-35]. When the particles were added to ANA1 cells or NIH3T3 cells, MTS indicated that there was generally minimal cytotoxicity. Over 80% cell viability was observed when cells were cultured with different concentrations of FLUO-OVA-GAL-LDL nanoparticles (Figure 4), indicating the low cytotoxicity of the particles and highlighting their potential for in vivo, as well as in vitro antigen delivery.

Uptake of FLUO-OVA-GAL-LDL nanoparticle by ANA1 and NIH3T3 cells

To test the preferential uptake of the FLUO-OVA-GAL-LDL nanoparticles by macrophages rather than other cells, fluorescence microscopy and flow cytometry studies were performed using the murine macrophage-like cell line ANA1, and the murine fibroblastic cell line NIH3T3. As expected, fluorescent microscopic images showed strong accumulation of FLUO-OVA-GAL-LDL as green fluorescence spots in the peri-nuclear region in the cytoplasm of ANA1 cells (Figure 5Ad). In contrast, free FLUO-OVA showed much less accumulation in the perinuclear region of ANA1 cells (Figure 5Aa). In sharp contrast to the strong accumulation of FLUO-OVA-GAL-LDL in ANA1 cells, no accumulation of FLUO-OVA-GAL-LDL was observed in NIH3T3 cells (Figure 5Bj), indicating the specific targeting effect of galactosylated LDL nanoparticles. Similarly, there was also no accumulation of FLUO-OVA in NIH3T3 cells (Figure 5Bg). Once taken up into ANA1 cells, the antigen FLUO-OVA was internalized and localized in cytoplasmic compartments, possibly endosomes/lysosomes, providing the opportunity for antigen to be degraded, transferred to the cytosol, processed to form a complex with MHC class I molecules, and then presented to OVA specific OT-1 T cells. This was consistent with the previous report that ligands taken up via the galactose-particle receptor entered KCs via the endosomal-lysosomal route[36]. In the fluorescence microscopic study, we used the ratio of 10:500:1:600 ratio rather than 10:5000:1:600 because even this ratio with potential lower galactosylation ratio was enough to show the preferable uptake of FLUO-OVA-GAL-LDL by ANA1 cells, indicating the efficiency of enhancement of FLUO-OVA uptake by ANA1 cells with the help of galactosylated LDL.

Figure 6A shows the mean fluorescence intensity (MFI) of ANA1 cells or NIH3T3 cells that were incubated for 5h with four formulations of FLUO-OVA-GAL-LDL nanoparticles at a dose corresponding to 2 μg/mL of FLUO-OVA, or the equivalent dose of free FLUO-OV. This MFI measurement represents the amount of FLUO-OVA taken up by the cells. The four formulations of FLUO-OVA-GAL-LDL nanoparticles were prepared using different molar ratios of FLUO-OVA: lactobionic acid: LDL: EDC in the synthesis reaction, as indicated in Figure 6A. As shown in Figure 6A, the MFI of ANA1 cells that were incubated for 5h with

NIH-PA Author Manuscript

NIH-PA Author Manuscript

NIH-PA Author Manuscript

FLUO-OVA-GAL-LDL nanoparticles was greater than after incubation with free FLUO-OVA. This enhancement of FLUO-OVA uptake by FLUO-OVA-GAL-LDL nanoparticles was in agreement with the microscopic results shown in Figure 5. Figure 6A also shows that increasing the molecular ratio of lactobionic acid, with the potential to increase the galactosylated moiety, increased the uptake of FLUO-OVA-GAL-LDL by ANA1 cells. This selectivity might have been due to the higher expression of GPr on macrophages. We chose the ratio of 10:5000:1:600 as the optimized formulation rather than 10:50000:1:600 because Figure 6 (A) and (C) show that using the formulation with the ratio of 10:50000:1:600, the MFI also increased in both non-target cell population, the NIH3T3 cells and hepatic stellate cells. We were not interested only in the most effective uptake, but also in the most effective discrimination between macrophages and other cells. Nanoparticles made using the 10:5000:1:600 conjugation ratios gave both good uptake, and good macrophage selectivity. Thus we chose the ratio of 10:5000:1:600 as our optimal formulation.

Using the optimal formulation, an approximate 7-fold increase in uptake by ANA1 cells was observed with FLUO-OVA-GAL-LDL nanoparticles (MFI=100.56) over free FLUO-OVA (MFI=14.62). At the same time, there was very little increase in NIH3T3 cell uptake with FLUO-OVA-GAL-LDL nanoparticles over free FLUO-OVA (Figure 6A), revealing the targeting properties of the FLUO-OVA-GAL-LDL nanoparticles to macrophage-like ANA1 cells, rather than NIH3T3 cells. For the optimal formulation with the reaction molar ratio of 10:5000:1:600 (FLUO-OVA: Lactobionic acid: LDL: EDC), FLUO-OVA-GAL-LDL nanoparticles resulted in an approximate 7-fold increase of uptake in ANA1 cells (MFI=100.56) than in NIH3T3 cells (MFI=14.87). However, uptake of free FLUO-OVA was essentially the same in the two cell lines (MFI of 14.62 for ANA1 cells, versus 12.42 for NIH3T3 cells). This confirms quantitatively the above microscopic results that FLUO-OVA-GAL-LDL nanoparticles were preferentially taken up by macrophage like ANA1 cells, rather than fibroblastic NIH3T3 cells.

Evaluation of mechanism of uptake of FLUO-OVA-GAL-LDL nanoparticles

To evaluate the mechanism of uptake of FLUO-OVA-GAL-LDL nanoparticles by macrophages, flow cytometric experiments were performed using ANA1 cells. As shown in Figure 6B, with the pretreatment of PBS for 45 min, a higher MFI was observed in the flow cytometric assay of ANA 1 cells after incubation for 5h with FLUO-OVA-GAL-LDL nanoparticles at a dose corresponding to 1.5 μg/mL of FLUO-OVA over incubation with an equivalent dose of free FLUO-OVA. This fluorescent signal was significantly inhibited by pretreatment of 10-fold GAL-LDL, but not by pretreatment of 10-fold LDL, consistent with blocking of the GPr, but not the LDL receptor. However, pretreatment of neither 10-fold of GAL-LDL nor 10-fold of LDL had an inhibitory effect on the uptake of free FLUO-OVA. Taken together, these data suggest that FLUO-OVA-GAL-LDL in ANA1 cells was taken up through the GPr, rather than the LDL receptor; however free FLUO-OVA were taken up by another mechanism. We interpret this experiment on the basis that, during the pretreatment of GAL-LDL, the galactosylated nanoparticles would occupy the GPr, and this would result in the decreased uptake of FLUO-OVA via FLUO-OVA-GAL-LDL. However, this experiment must be interpreted with caution because we have not yet identified a specific GPr inhibitor. Targeting of the kind we envisage is exemplified by the work of Zheng et al, who demonstrated that folic acid conjugation to the Lys side-chain amino groups blocks binding to the normal LDL receptor, and re-routes the resulting conjugate to cancer cells through their folate receptor[15].

NIH-PA Author Manuscript

NIH-PA Author Manuscript

NIH-PA Author Manuscript

Uptake of FLUO-OVA-GAL-LDL Nanoparticles by Primary Peritoneal Macrophages versus Primary Hepatic Stellate Cells

The long-term goal of these studies is to deliver antigens or drugs selectively to KCs in vivo. Therefore it was important to substantiate the results in primary cells. Therefore, the cellular uptake of FLUO-OVA was further studied in primary peritoneal macrophages and primary hepatic stellate cells. As can be seen in Figure 6C, the optimal formulation of FLUO-OVA-GAL-LDL nanoparticles resulted in a 6-fold increase in the level of uptake of FLUO-OVA in peritoneal macrophages (MFI=53.22) over free FLUO-OVA (MFI=8.35). Secondly, these nanoparticles resulted in an approximately 12-fold increase in the level of uptake of FLUO-OVA in peritoneal macrophages (MFI=53.22), compared to hepatic stellate cells (MFI=4.24). This suggested that the targeting properties of FLUO-OVA-GAL-LDL nanoparticles applied to peritoneal macrophages, rather than hepatic stellate cells. Thirdly, similar to what was seen in ANA1 cells, with the increase of galactosylation ratio, FLUO-OVA-GAL-LDL nanoparticles enhanced the uptake of FLUO-OVA by peritoneal macrophages, consistent with the uptake of FLUO-OVA-GAL-LDL through the GPr. Fourthly, similar to that seen in NIH3T3 cells, FLUO-OVA-GAL-LDL did not result in a significant increase of FLUO-OVA uptake by hepatic stellate cells over free FLUO-OVA. Furthermore, increase of the galactosylation ratio during the synthesis of FLUO-OVA-GAL-LDL nanoparticles did not increase their uptake by stellate cells. This study confirms that that FLUO-OVA-GAL-LDL nanoparticles can target specifically to primary peritoneal macrophages, rather than hepatic stellate cells. With the increase of galactosylation ratio, the FLUO-OVA-GAL-LDL nanoparticles can enhance the uptake of FLUO-OVA not only in macrophage-like cell lines, but also in normal, primary peritoneal macrophages. This reveals the potential of FLUO-OVA-GAL-LDL nanoparticles for use as carriers for targeted delivery of loaded antigen to KCs in the liver, but not to HSC.

Enhanced MHC Class I Antigen Presentation to OVA Specific OT.1 T Cells by FLUO-OVA-GAL-LDL Nanoparticles

To test whether the FLUO-OVA loaded FLUO-OVA-GAL-LDL nanoparticles could deliver OVA to Antigen Presenting Cells (APC) and subsequently activate OVA specific OT-1 T cells, macrophages were harvested from the peritoneal cavity of C57/BL6 mice. These cells, maintained as an adherent monolayer, were first pulsed with FLUO-OVA-GAL-LDL nanoparticles or free FLUO-OVA for 14 h, and then cultured for 5 days with transgenic OT-1 $CD8^+$ T lymphocytes that had been stained with the dye, CFSE. This dye acts as an indicator of cell division, since it stains resting lymphocytes brightly, forming a unimodal peak of fluorescence on FACS analysis. Cell proliferation dilutes the level of staining two fold with each division cycle. Figure 7A shows that at a dosage from 2 μg/mL to 20 μg/mL of FLUO-OVA, OT-1 T cell proliferation gradually increased when peritoneal macrophages were pulsed with FLUO-OVA-GAL-LDL nanoparticles (made using a molar ratio is 150:5000:1 for FLUO-OVA: Lactobionic acid: LDL) or free FLUO-OVA. As compared with free FLUO-OVA at a dose of 20 μg/mL, the equivalent dose of FLUO-OVA-GAL-LDL nanoparticles enhanced the extent of OT-1 T cell proliferation almost 7-fold, as can be seen from the percentage of divided OT-1 T cells ($V\alpha2^+CD8^+$ cells) in Figure 7A and Figure 7B. As a positive control, peritoneal macrophages were pulsed with 1.5 μg/mL of OVA peptide SIINFEKL before OT-1 T cell addition. Pre-incubation with PBS or native LDL did not cause OT-1 T cell proliferation. These results demonstrated the successful delivery of FLUO-OVA as an antigen to APC by FLUO-OVA-GAL-LDL nanoparticles, and also revealed that FLUO-OVA-GAL-LDL nanoparticles as an OVA delivery system enhances OVA-specific OT-1 T cell proliferation and division as compared to free FLUO-OVA.

The conjugation of FLUO-OVA and the galactose moiety with LDL worked well and the bioactivities of both antigen and galactose particle ligand remained. The increase of OT-1 T

NIH-PA Author Manuscript

NIH-PA Author Manuscript

NIH-PA Author Manuscript

cell response induced by FLUO-OVA-GAL-LDL nanoparticles is likely to be because of the enhanced uptake of antigen by the macrophages. This was consistent with the previous report that formulating an antigen in particulate carriers could increase the immune response[37] .

As was shown in the mechanistic studies, FLUO-OVA-GAL-LDL was possibly internalized in macrophages via GPr receptor, and then might be processed via the endocytic pathway. The use of galactosylated LDL as an OVA-delivery vehicle indeed reduced the threshold of OVA concentration required for effective MHC class I presentation by primary peritoneal macrophages. Since the antigen-specific OT-1 $CD8^+$ T cells will undergo rapid proliferation only upon recognition of their cognate antigen[38], we conclude that FLUO-OVA-GAL-LDL nanoparticles are a good antigen delivery system to target macrophages.

Typically, exogenously administered proteins do not efficiently enter the cytosol because of poor permeability across the plasma membrane and endosomal/ lysosomal membrane. Instead, after uptake by cells through endocytosis, they are typically degraded in the endosomal/ lysosomal compartment and thus presented predominantly in a MHC class II-restricted manner [39]. In our study, enhanced MHC Class I antigen presentation to OVA specific OT-1 T cells was observed by FLUO-OVA-GAL-LDL nanoparticles. Some other studies also showed that professional APCs such as dendritic cells or macrophages were able to present some exogenous antigens on MHC class I [40]. This involves the transportation of internalized antigens from the endosome/lysome to the cytosol for MHC class I presentation[41, 42]. As shown before, efficient MHC class I presentation by macrophages was found after induction of macropinocytosis at high antigen concentrations[43], after artificial endosomal fusion by pH-sensitive liposomes[44] or after endosomal disruption by Listeriolysin O-containing liposomes[45, 46] or when antigens were coupled to pH-sensitive polymeric particles[47] etc. It is, therefore, possible that high antigen concentrations or interaction of the FLUO-OVA-GAL-LDL nanoparticles with phagosomal membranes facilitated antigen delivery to the cytosol by inducing leakage from endocytic compartments[44-47]; alternatively such leakage could possibly occur simply because of overload[48]. Whatever the mechanism, the increased internalization of antigen with the aid of FLUO-OVA-GAL-LDL nanoparticles compared with free FLUO-OVA also contributed to the enhanced MHC Class I antigen presentation to OVA specific OT-1 T Cells.

In conclusion, we demonstrated in the present study that the conjugation of FLUO-OVA and lactobionic acid with LDL resulted in a substantially increased uptake of OVA by murine macrophage-like ANA1 cells, and also by primary peritoneal macrophages, over murine fibroblast NIH3T3 cells and primary hepatic stellate cells respectively. With the increase of galactosylation ratio, the uptake increased in ANA1 cells and peritoneal macrophages; blocking experiments suggest this may be due to the engagement of the GPr on the surface of those cells. Compared with free FLUO-OVA, a 7-fold increase of OT-1 T cell proliferation was observed when they were co-cultured with peritoneal macrophages pulsed with FLUO-OVA loaded galactosylated LDL at a dose of 20 μg/mL OVA. This antigen delivery system could be used for targeting KCs in the liver, to address the question of the role of this antigen presenting cell in liver immunology or as an alternative way of delivering drug or vaccine directly at macrophages.

Acknowledgments

The authors thank Dr. Jim Miller for assistance with deconvolution microscopy. We also thank Karen L. de Mesy Bentley for her assistance with TEM images. This work was supported by NIH grant AI064463 to I. Nicholas Crispe.

References

(1). Mackay IR. Hepatoimmunology: a perspective. Immunol. Cell Biol 2002;80(1):36–44. [PubMed: 11869361]

NIH-PA Author Manuscript

NIH-PA Author Manuscript

NIH-PA Author Manuscript

(2). Racanelli V, Rehermann B. The liver as an immunological organ. Hepatology 2006;43(2 Suppl 1):S54–62. [PubMed: 16447271]

(3). Bertolino P, McCaughan GW, Bowen DG. Role of primary intrahepatic T-cell activation in the 'liver tolerance effect'. Immunol. Cell Biol 2002;80(1):84–92. [PubMed: 11869365]

(4). Dong L, Zuo L, Xia S, Gao S, Zhang C, Chen J, Zhang J. Reduction of liver tumor necrosis factor-alpha expression by targeting delivery of antisense oligonucleotides into Kupffer cells protects rats from fulminant hepatitis. J. Gene Med 2009;11(3):229–239. [PubMed: 19189285]

(5). van Rooijen N. Liposomes for targeting of antigens and drugs: immunoadjuvant activity and liposome-mediated depletion of macrophages. J. Drug Target 2008;16(7):529–534. [PubMed: 18686122]

(6). Sun X, Wu F, Lu W, Zhang ZR. Sustained-release hydroxycamptothecin polybutylcyanoacrylate nanoparticles as a liver targeting drug delivery system. Pharmazie 2004;59(10):791–794. [PubMed: 15544059]

(7). Yang SC, Bhide M, Crispe IN, Pierce RH, Murthy N. Polyketal copolymers: a new acid-sensitive delivery vehicle for treating acute inflammatory diseases. Bioconjug. Chem 2008;19(6):1164–1169. [PubMed: 18500834]

(8). Ahsan F, Rivas IP, Khan MA, Torres Suarez AI. Targeting to macrophages: role of physicochemical properties of particulate carriers--liposomes and microspheres--on the phagocytosis by macrophages. J. Control. Release 2002;79(13):29–40. [PubMed: 11853916]

(9). Kohler N, Sun C, Wang J, Zhang M. Methotrexate-modified superparamagnetic nanoparticles and their intracellular uptake into human cancer cells. Langmuir 2005;21(19):8858–8864. [PubMed: 16142971]

(10). Liu TC, Wang JH, Wang HQ, Zhang HL, Zhang ZH, Hua XF, Cao YC, Zhao YD, Luo QM. Bioconjugate recognition molecules to quantum dots as tumor probes. J. Biomed. Mater. Res. A 2007;83A(4):1209–1216. [PubMed: 17600337]

(11). Ding H, Yong K-T, Roy I, Pudavar HE, Law WC, Bergey EJ, Prasad PN. Gold Nanorods Coated with Multilayer Polyelectrolyte as Contrast Agents for Multimodal Imaging. J. Phys. Chem. C 2007;111(34):12552–12557.

(12). Tekle C, Deurs B. v. Sandvig K, Iversen T-G. Cellular Trafficking of Quantum Dot-Ligand Bioconjugates and Their Induction of Changes in Normal Routing of Unconjugated Ligands. Nano. Letters 2008;8(7):1858–1865. [PubMed: 18570482]

(13). Chavanpatil MD, Khdair A, Panyam J. Nanoparticles for cellular drug delivery: mechanisms and factors influencing delivery. J. Nanosci. Nanotechnol 2006;6(910):2651–2663. [PubMed: 17048473]

(14). Paul M, Durand R, Boulard Y, Fusai T, Fernandez C, Rivollet D, Deniau M, Astier A. Physicochemical characteristics of pentamidine-loaded polymethacrylate nanoparticles: implication in the intracellular drug release in Leishmania major infected mice. J. Drug Target 1998;5(6):481–490. [PubMed: 9783679]

(15). Zheng G, Chen J, Li H, Glickson JD. Rerouting lipoprotein nanoparticles to selected alternate receptors for the targeted delivery of cancer diagnostic and therapeutic agents. Proc. Natl. Acad. Sci. U S A 2005;102(49):17757–17762. [PubMed: 16306263]

(16). Chen J, Corbin IR, Li H, Cao W, Glickson JD, Zheng G. Ligand conjugated low-density lipoprotein nanoparticles for enhanced optical cancer imaging in vivo. J. Am. Chem. Soc 2007;129(18):5798–5799. [PubMed: 17428054]

(17). Vyas SP, Sihorkar V. Endogenous carriers and ligands in non-immunogenic site-specific drug delivery. Adv. Drug Deliv. Rev 2000;43(23):101–164. [PubMed: 10967224]

(18). Bijsterbosch MK, Manoharan M, Dorland R, Waarlo IH, Biessen EA, van Berkel TJ. Delivery of cholesteryl-conjugated phosphorothioate oligodeoxynucleotides to Kupffer cells by lactosylated low-density lipoprotein. Biochem. Pharmacol 2001;62(5):627–633. [PubMed: 11585059]

(19). Popielarski SR, Hu-Lieskovan S, French SW, Triche TJ, Davis ME. A nanoparticle-based model delivery system to guide the rational design of gene delivery to the liver. 2. In vitro and in vivo uptake results. Bioconjug. Chem 2005;16(5):1071–1080. [PubMed: 16173782]

NIH-PA Author Manuscript

NIH-PA Author Manuscript

NIH-PA Author Manuscript

(20). Pitas RE, Boyles J, Mahley RW, Bissell DM. Uptake of chemically modified low density lipoproteins in vivo is mediated by specific endothelial cells. J. Cell Biol 1985;100(1):103–117. [PubMed: 3965468]

(21). Benten D, Follenzi A, Bhargava KK, Kumaran V, Palestro CJ, Gupta S. Hepatic targeting of transplanted liver sinusoidal endothelial cells in intact mice. Hepatology 2005;42(1):140–148. [PubMed: 15918158]

(22). Yong KT, Qian J, Roy I, Lee HH, Bergey EJ, Tramposch KM, He S, Swihart MT, Maitra A, Prasad PN. Quantum rod bioconjugates as targeted probes for confocal and two-photon fluorescence imaging of cancer cells. Nano. Lett 2007;7(3):761–765. [PubMed: 17288490]

(23). Xu G, Yong KT, Roy I, Mahajan SD, Ding H, Schwartz SA, Prasad PN. Bioconjugated quantum rods as targeted probes for efficient transmigration across an in vitro blood-brain barrier. Bioconjug. Chem 2008;19(6):1179–1185. [PubMed: 18473444]

(24). Gao S, Chen J, Xu X, Ding Z, Yang YH, Hua Z, Zhang J. Galactosylated low molecular weight chitosan as DNA carrier for hepatocyte-targeting. Int. J. Pharm 2003;255(12):57–68. [PubMed: 12672602]

(25). Konnings S, Copland MJ, Davies NM, Rades T. A method for the incorporation of ovalbumin into immune stimulating complexes prepared by the hydration method. Int. J. Pharm 2002;241(2):385–389. [PubMed: 12100866]

(26). Law W-C, Yong K-T, Roy I, Xu G, Ding H, Bergey EJ, Zeng H, Prasad PN. Optically and Magnetically Doped Organically Modified Silica Nanoparticles as Efficient Magnetically Guided Biomarkers for Two-Photon Imaging of Live Cancer Cells. J. Phys. Chem. C 2008;112(21):7972–7977.

(27). Bonoiu AC, Mahajan SD, Ding H, Roy I, Yong KT, Kumar R, Hu R, Bergey EJ, Schwartz SA, Prasad PN. Nanotechnology approach for drug addiction therapy: gene silencing using delivery of gold nanorod-siRNA nanoplex in dopaminergic neurons. Proc. Natl. Acad. Sci. U S A 2009;106(14):5546–5550. [PubMed: 19307583]

(28). Kim JG, Keshava C, Murphy AA, Pitas RE, Parthasarathy S. Fresh mouse peritoneal macrophages have low scavenger receptor activity. J. Lipid Res 1997;38(11):2207–2215. [PubMed: 9392418]

(29). Ebrahimkhani MR, Kiani S, Oakley F, Kendall T, Shariftabrizi A, Tavangar SM, Moezi L, Payabvash S, Karoon A, Hoseininik H, Mann DA, Moore KP, Mani AR, Dehpour AR. Naltrexone, an opioid receptor antagonist, attenuates liver fibrosis in bile duct ligated rats. Gut 2006;55(11):1606–1616. [PubMed: 16543289]

(30). Wuensch SA, Pierce RH, Crispe IN. Local intrahepatic CD8+ T cell activation by a non-self-antigen results in full functional differentiation. J. Immunol 2006;177(3):1689–97. [PubMed: 16849478]

(31). Ghosh S, Saxena RK. Early effect of Mycobacterium tuberculosis infection on Mac-1 and ICAM-1 expression on mouse peritoneal macrophages. Exp. Mol. Med 2004;36(5):387–395. [PubMed: 15557811]

(32). Donnini A, Argentati K, Mancini R, Smorlesi A, Bartozzi B, Bernardini G, Provinciali M. Phenotype, antigen-presenting capacity, and migration of antigen-presenting cells in young and old age. Exp. Gerontol 2002;37(89):1097–112. [PubMed: 12213560]

(33). Hu R, Yong K-T, Roy I, Ding H, He S, Prasad PN. Metallic Nanostructures as Localized Plasmon Resonance Enhanced Scattering Probes for Multiplex Dark-Field Targeted Imaging of Cancer Cells. J. Phys. Chem. C 2009;113(7):2676–2684.

(34). Lee CH, Chou TC, Su TL, Yu J, Shao LE, Yu AL. BO-0742, a derivative of AHMA and N-mustard, has selective toxicity to drug sensitive and drug resistant leukemia cells and solid tumors. Cancer Lett 2009;276(2):204–211. [PubMed: 19108949]

(35). Yong KT, Ding H, Roy I, Law WC, Bergey EJ, Maitra A, Prasad PN. Imaging pancreatic cancer using bioconjugated InP quantum dots. ACS Nano 2009;3(3):502–510. [PubMed: 19243145]

(36). Bijsterbosch MK, Ziere GJ, Van Berkel TJ. Lactosylated low density lipoprotein: a potential carrier for the site-specific delivery of drugs to Kupffer cells. Mol. Pharmacol 1989;36(3):484–489. [PubMed: 2550781]

(37). Friede M, Aguado MT. Need for new vaccine formulations and potential of particulate antigen and DNA delivery systems. Adv. Drug Deliv. Rev 2005;57(3):325–331. [PubMed: 15560944]

NIH-PA Author Manuscript

NIH-PA Author Manuscript

NIH-PA Author Manuscript

(38). Isogawa M, Furuichi Y, Chisari FV. Oscillating CD8(+) T cell effector functions after antigen recognition in the liver. Immunity 2005;23(1):53–63. [PubMed: 16039579]

(39). Stier EM, Mandal M, Lee KD. Differential cytosolic delivery and presentation of antigen by listeriolysin O-liposomes to macrophages and dendritic cells. Mol. Pharm 2005;2(1):74–82. [PubMed: 15804180]

(40). Gurnani K, Kennedy J, Sad S, Sprott GD, Krishnan L. Phosphatidylserine receptor-mediated recognition of archaeosome adjuvant promotes endocytosis and MHC class I cross-presentation of the entrapped antigen by phagosome-to-cytosol transport and classical processing. J. Immunol 2004;173(1):566–578. [PubMed: 15210818]

(41). Rodriguez A, Regnault A, Kleijmeer M, Ricciardi-Castagnoli P, Amigorena S. Selective transport of internalized antigens to the cytosol for MHC class I presentation in dendritic cells. Nat. Cell Biol 1999;1(6):362–368. [PubMed: 10559964]

(42). Homhuan A, Kogure K, Nakamura T, Shastri N, Harashima H. Enhanced antigen presentation and CTL activity by transduction of mature rather than immature dendritic cells with octaarginine-modified liposomes. J. Control. Release 2009;136(1):79–85. [PubMed: 19344678]

(43). Norbury CC, Hewlett LJ, Prescott AR, Shastri N, Watts C. Class I MHC presentation of exogenous soluble antigen via macropinocytosis in bone marrow macrophages. Immunity 1995;3(6):783–791. [PubMed: 8777723]

(44). Nakamura T, Moriguchi R, Kogure K, Shastri N, Harashima H. Efficient MHC class I presentation by controlled intracellular trafficking of antigens in octaarginine-modified liposomes. Mol. Ther 2008;16(8):1507–1514. [PubMed: 18560420]

(45). Mandal M, Kawamura KS, Wherry EJ, Ahmed R, Lee KD. Cytosolic delivery of viral nucleoprotein by listeriolysin O-liposome induces enhanced specific cytotoxic T lymphocyte response and protective immunity. Mol. Pharm 2004;1(1):2–8. [PubMed: 15832496]

(46). Lee KD, Oh YK, Portnoy DA, Swanson JA. Delivery of macromolecules into cytosol using liposomes containing hemolysin from Listeria monocytogenes. J. Biol. Chem 1996;271(13):7249–7252. [PubMed: 8631734]

(47). Bachelder EM, Beaudette TT, Broaders KE, Paramonov SE, Dashe J, Frechet JM. Acid-degradable polyurethane particles for protein-based vaccines: biological evaluation and in vitro analysis of particle degradation products. Mol. Pharm 2008;5(5):876–884. [PubMed: 18710254]

(48). Kovacsovics-Bankowski M, Rock KL. A phagosome-to-cytosol pathway for exogenous antigens presented on MHC class I molecules. Science 1995;267(5195):243–246. [PubMed: 7809629]

NIH-PA Author Manuscript
NIH-PA Author Manuscript
NIH-PA Author Manuscript

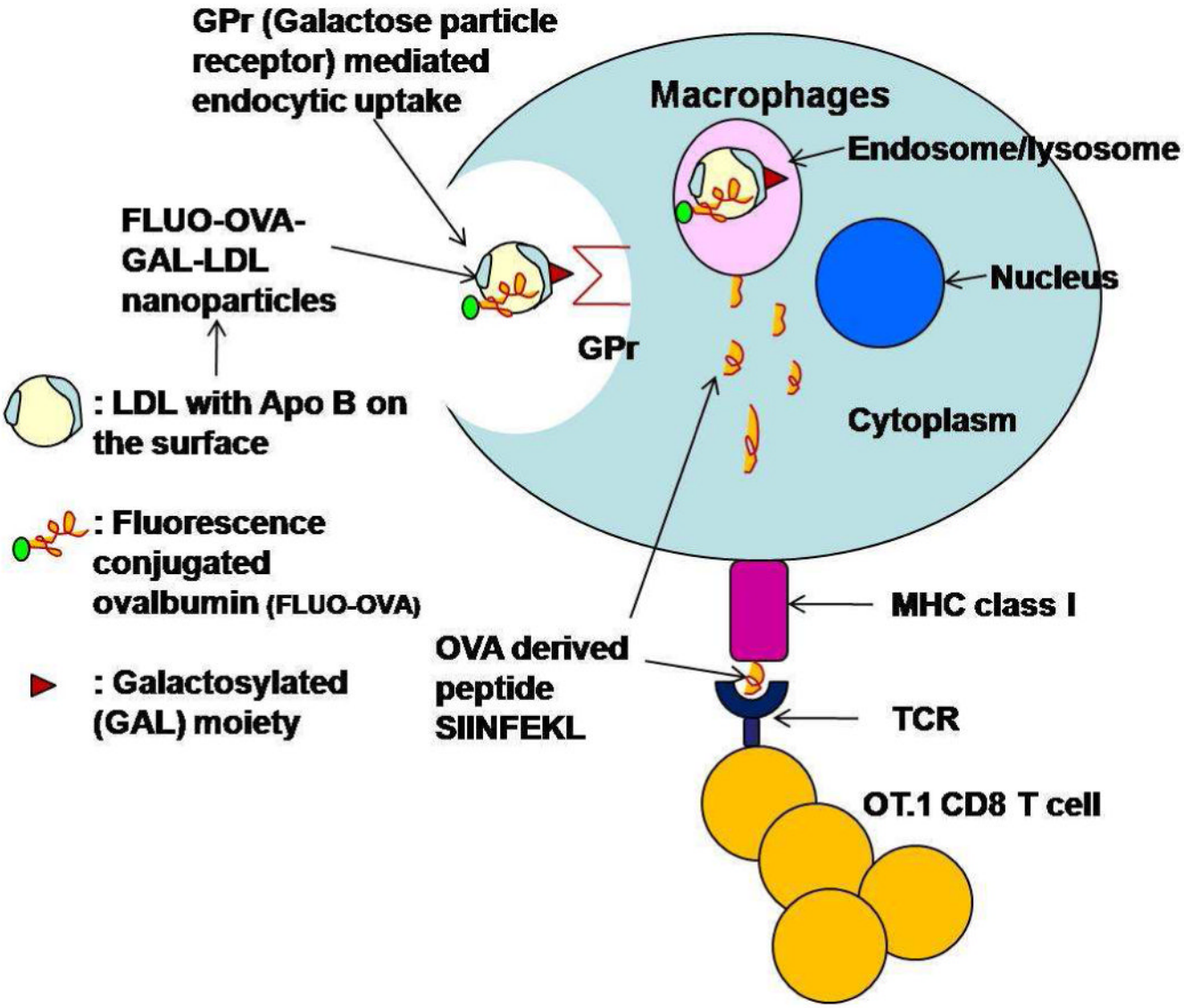

Figure 1.

Mechanism of uptake of FLUO-OVA-GAL-LDL nanoparticles. The scheme represents localization of FLUO-OVA-GAL-LDL in endosomes/lysosomes after internalization through the GPr (galactose particle receptor) endocytosis pathway. Then the antigen OVA is degraded and transferred to the cytosol, processed to form a complex with MHC class I molecules, and subsequently presented to OVA specific OT-1 T cells, resulting in their proliferation.

NIH-PA Author Manuscript

NIH-PA Author Manuscript

NIH-PA Author Manuscript

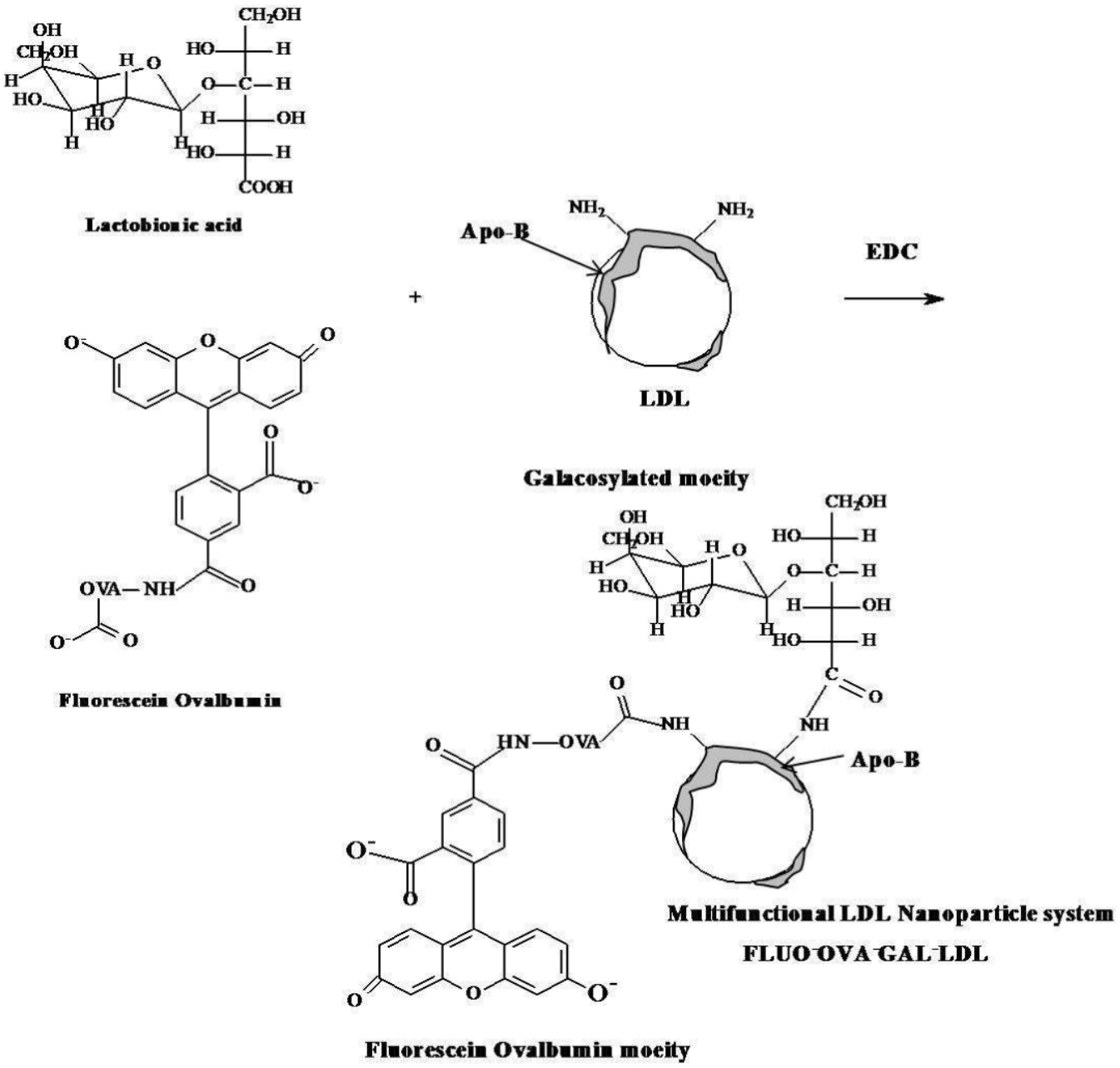

Figure 2.
Scheme of the conjugation method for the preparation of FLUO-OVA-GAL-LDL nanoparticles.

NIH-PA Author Manuscript

NIH-PA Author Manuscript

NIH-PA Author Manuscript

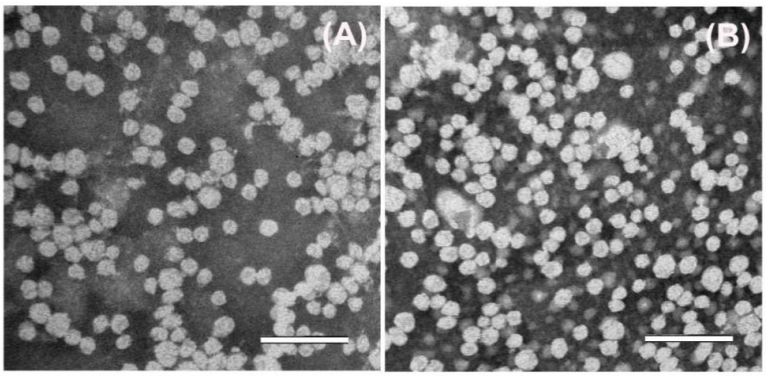

Figure 3.
TEM images of (A) native LDL (B) FLUO-OVA-GAL-LDL nanoparticles, scale bar=100 nm.

NIH-PA Author Manuscript
NIH-PA Author Manuscript
NIH-PA Author Manuscript

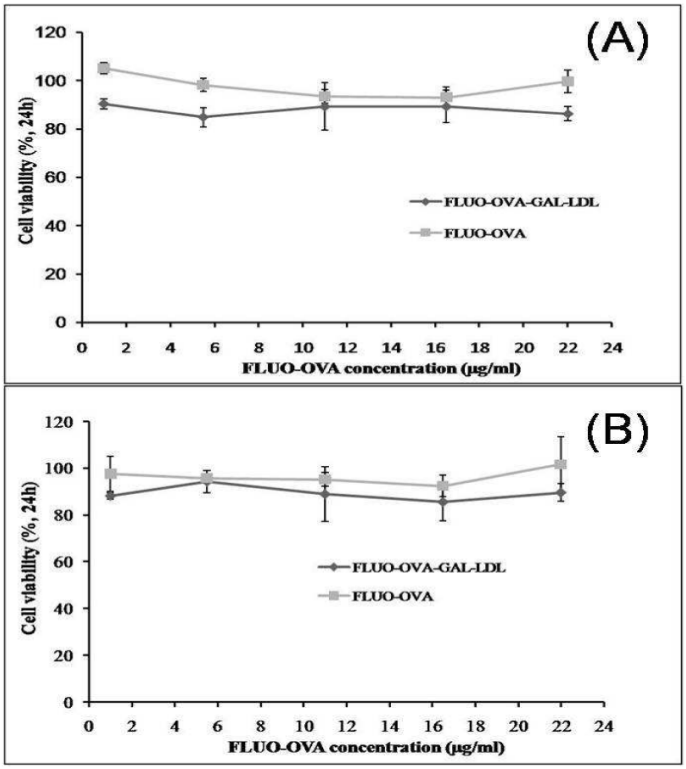

Figure 4.

Cytotoxicity of FLUO-OVA-GAL-LDL towards ANA1 cells (A) and NIH3T3 cells (B). The ANA1 cells or NIH3T3 cells were treated with FLUO-OVA-GAL-LDL nanoparticles at different OVA concentration, or with free FLUO-OVA. Relative cell viability was expressed as a percentage of that in control cells treated with media alone. Comparable to free FLUO-OVA, FLUO-OVA-GAL-LDL showed minimal cytotoxicity towards either cell line after 24 h of incubation treatment.

NIH-PA Author Manuscript

NIH-PA Author Manuscript

NIH-PA Author Manuscript

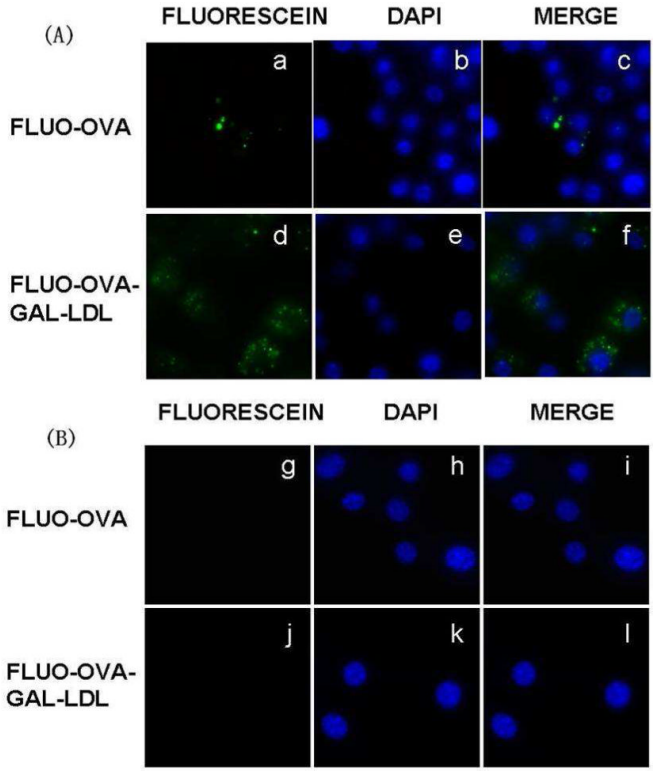

Figure 5.

Specific delivery of FLUO-OVA-GAL-LDL to ANA1 cells. Representative fluorescent micrographs of FLUO-OVA visualized by fluorescein (green, a, d, g, j) demonstrate FLUO-OVA uptake by ANA1 cells (A) and lack of such uptake by NIH3T3 cells (B) after 5 h of incubation. The DNA in nuclei was stained with DAPI (blue, b, e, h, k). Micrographs c, f, i and l are the merge images of the fluorescein and DAPI images on the same row.

NIH-PA Author Manuscript

NIH-PA Author Manuscript

NIH-PA Author Manuscript

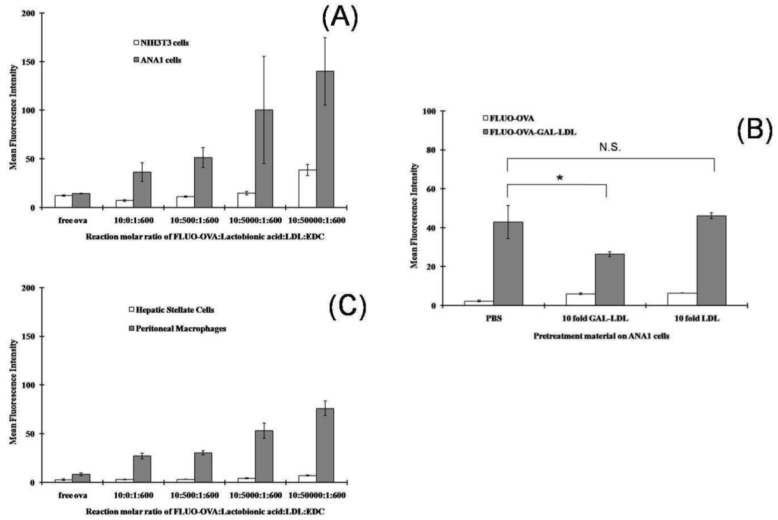

Figure 6.

(A) Mean fluorescence intensity measured by flow cytometry to indicate the uptake of FLUO-OVA by ANA1 cells or NIH3T3 cells after 5 h incubation with 2 μg/mL of free FLUO-OVA or with FLUO-OVA-GAL-LDL, made using different galactosylation ratios. (B) The uptake of FLUO-OVA-GAL-LDL was inhibited by a 10-fold excess of GAL-LDL relative to a PBS control, but not by a 10-fold excess of LDL. The MFI of fluorescence was compared in ANA1 cells treated with FLUO-OVA-GAL-LDL after pretreatment with either PBS, or GAL-LDL, or LDL alone. The significances of the differences were evaluated using ANOVA test. Results are expressed as average values ±S.D. from three independent experiments. Significant differences with $P<0.05$ are indicated *, while N.S. indicates no significant difference. (C) Mean fluorescence intensity measured by flow cytometry to indicate the uptake of FLUO-OVA by primary peritoneal macrophages or hepatic stellate cells after 5 h incubation with 2 μg/mL of free FLUO-OVA, versus FLUO-OVA-GAL-LDL prepared using different galactosylation ratios.

NIH-PA Author Manuscript

NIH-PA Author Manuscript

NIH-PA Author Manuscript

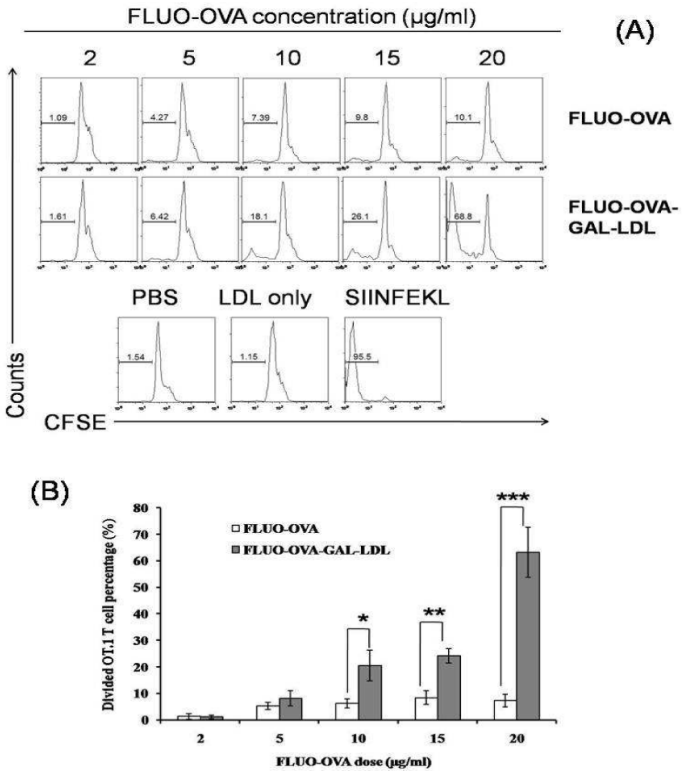

Figure 7.

(A) Representative histogram of CFSE-labeled OT-1 T cells after 5 days of co-culture with peritoneal macrophages pulsed for 14h with different dose of FLUO-OVA or FLUO-OVA-GAL-LDL nanoparticles. Histograms are gated on $V\alpha2^{+}CD8^{+}$ cells. Proliferation was detected as dilution of CFSE on OT-1 cells. Control wells were pulsed with PBS, LDL or SINFEKL before OT-1 cell addition. (B) Percentage of divided OT-1 T cell obtained after 5 days of co-culture with peritoneal macrophages pulsed for 14h with different dose of FLUO-OVA or FLUO-OVA-GAL-LDL nanoparticles. Results are expressed as average values ±S.D. from three independent experiments. Significance of differences in the percentage of divided T cells, in response to macrophages treated with FLUO-OVA versus FLUO-OVA-GAL-LDL was determined using ANOVA test: *, $p<0.05$, **, $p<0.01$, ***, $p<0.001$.